Mon. Not. R. Astron. Soc. **000**, 000–000 (0000) Printed 4 June 2015 (MN LATEX style file v2.2)

Galaxy Zoo: Evidence for quenching caused by AGN feedback

R. J. Smethurst,[1] C. J. Lintott,[1] B. D. Simmons,[1]
[1] *Oxford Astrophysics, Department of Physics, University of Oxford, Denys Wilkinson Building, Keble Road, Oxford, OX1 3RH, UK*

4 June 2015

ABSTRACT

1 INTRODUCTION

Two of the most important issues in current astrophysical understanding are: (i) the co-evolution of galaxies and their central black holes and (ii) the effects, if any, of AGN feedback. There is an obvious relationship between the evolution of a central black hole and it's host galaxy, observed multiple times and commonly referred to as the Maggorian relationship (Magorrian et al. 1998; Marconi & Hunt 2003; Haring & Rix 2004). AGN feedback was first theorised as a mechanism for regulating star formation in simulations (Croton et al. 2006; Bower et al. 2006; Somerville et al. 2008) and some indirect evidence has been observed for both positive and negative feedback in various systems (see the comprehensive review from Fabian 2006).

The strongest observational evidence for this feedback is that the largest fraction of AGN are found in the green valley (Cowie & Barger 2008; Hickox et al. 2009; Schawinski et al. 2010), suggesting some link to the process of quenching star formation in order for a galaxy to progress from the blue cloud to the red sequence. However, the rate at which this quenching occurs and whether it is a significant effect on the galaxy population as a whole, how not been studied.

Here we present the first observational population study of AGN host galaxies with the use of a new PYTHON routine, STARPY, implementing a Bayesian method. Given a near ultra-violet (NUV) & optical colour of an observed galaxy and by utilising SSP models, STARPY can effectively model the SFH of a galaxy with two parameters.

We therefore aim to determine the following:

(i) Are galaxies currently hosting an AGN undergoing quenching?
(ii) If so, when and at what rate does this quenching occur?

This letter proceeds as follows. Section 2 contains a description of the sample data, and details of the Bayesian analysis of an exponentially declining star formation history model. Section 3 contains the results produced by this analysis, with Section 4 providing a detailed discussion and a summary of the results obtained. The zero points of all ugriz magnitudes are in the AB system and where necessary we adopt the WMAP Seven-Year Cosmological parameters (Jarosik et al. 2011) with $(\Omega_m,\ \Omega_\lambda,\ h) = (0.26, 0.73, 0.71)$.

2 DATA & METHODS

2.1 Galaxy Zoo 2

In this investigation we use visual classifications of galaxy morphologies from the Galaxy Zoo 2[1] citizen science project (Willett et al. 2013), which obtains multiple independent classifications for each optical galaxy image; the full question tree for each image is shown in Figure 1 of Willett et al. 2013.

The Galaxy Zoo 2 (GZ2) project consists of 304,022 images from the SDSS DR8 (a subset of those classified in Galaxy Zoo 1; GZ1) all classified by *at least* 17 independent users, with the mean number of classifications standing at ~ 42.

Further to this, we required NUV photometry from the GALEX survey, within which $\sim 42\%$ of the GZ2 sample were observed, giving a total sample size of 126,316 galaxies. The completeness of this subsample of GZ2 matched to GALEX is shown in Figure 2 of Smethurst et al. (2015) with the u-band absolute magnitude against redshift for this sample compared with the SDSS data set. Typical Milky Way L_* galaxies with $M_u \sim -20.5$ are still included in the GZ2 subsample out to the highest redshift of $z \sim 0.25$; however dwarf and lower mass galaxies are only detected at the lowest redshifts.

2.2 STARPY

STARPY is a PYTHON code which allows the user to derive the quenched star formation history (SFH) of a galaxy through a Bayesian Markov Chain Monte Carlo method with the input of two observed photometric colours, a redshift, and the use of the SSP models of Bruzual & Charlot (2003). The star formation history template is an exponential decline of the SFR and is described by two parameters $[t_q, \tau]$ where t_q

⋆ This investigation has been made possible by the participation of more than 250,000 users in the Galaxy Zoo project. Their contributions are individually acknowledged at `http://authors.galaxyzoo.org`

[1] `http://zoo2.galaxyzoo.org/`

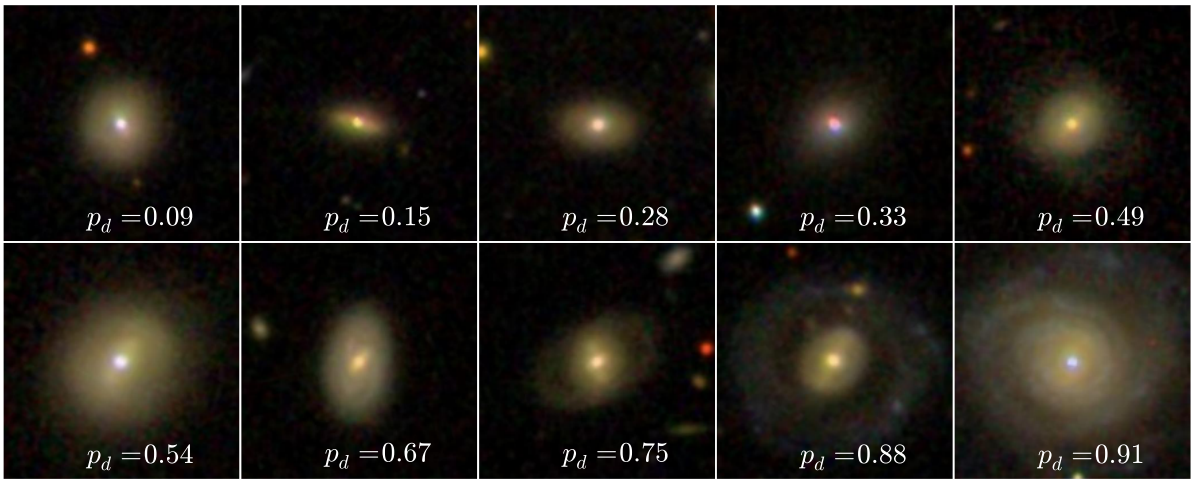

Figure 1. Randomly selected SDSS *gri* composite images from the sample of 984 Type 1 AGN showing the continuous probabilistic nature of the Galaxy Zoo sample from a redshift range $0.040 < z < 0.05$. The debiased 'disc or featured' vote fraction (see Willett et al. 2013) for each galaxy is shown. Note the bright point source of the AGN in the centre of each galaxy. The scale for each image is 0.099 arcsec/pixel.

is the time at which the onset of quenching begins [Gyr] and τ is the exponential rate at which quenching occurs [Gyr]. Under the simplifying assumption that all galaxies formed at $t = 0$ Gyr with an initial burst of star formation, the SFH can therefore be described as:

$$SFR = \begin{cases} i_{sfr}(t_q) & \text{if } t < t_q \\ i_{sfr}(t_q) \times exp\left(\frac{-(t-t_q)}{\tau}\right) & \text{if } t > t_q \end{cases} \quad (1)$$

where i_{sfr} is an initial constant star formation rate dependent on t_q (see Smethurst et al. 2015). A smaller τ value corresponds to a rapid quench, whereas a larger τ value corresponds to a slower quench. The output of STARPY is probabilistic in nature and provides the likelihood across the entirety of the two parameter space for each individual galaxy.

The probabilistic fitting methods to this SFH for an observed galaxy are described in full detail in Smethurst et al. (2015) wherein the STARPY code was run on a volume limited sample ($0.01 < z < 0.25$) of 126,316 galaxies of the Galaxy Zoo 2 project from SDSS DR8 (York et al. 2009; Aihara et al. 2011). This will be referred to as the GZ2-STARPY sample.

2.3 AGN Sample

We utilise a new sample of type 1 AGN selected by Oh et al. (2015) who built on the selection techniques of the OSSY catalogue[2] (Oh et al. 2011). To search for broad line region (BLR) AGN Oh et al. (2015) used a flux ratio between between two regions near the $H\alpha$ emission line in SDSS DR7 spectra. The two regions were $6460 - 6480\mathring{A}$ and $6523 - 6543\mathring{A}$ to give a flux ratio, F_{6533}/F_{6470}; which identified, if high, those candidate AGN host galaxies. Each spectra was

[2] http://gem.yonsei.ac.kr/ossy/

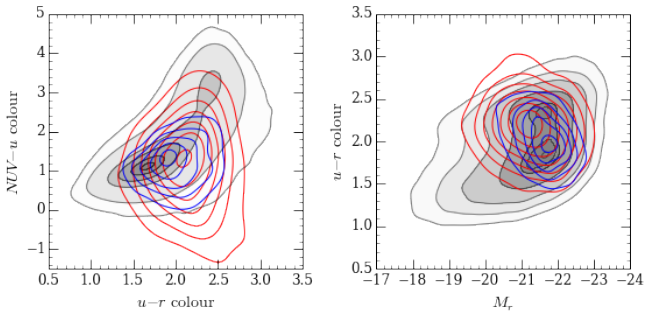

Figure 2. Optical-NUV colour-colour diagram (left panel) and optical colour-magnitude diagram (right panel) showing the inactive sample of galaxies (grey filled contours) in comparison to those for the AGN host galaxies with disc morphologies (blue contours; $p_d > 0.5$) and smooth morphologies (red contours; $p_d > 0.5$) with magnitudes corrected for the AGN flux contribution.

fit using the IDL PPXF and GANDALF programs with the Bruzual & Charlot (2003) and MILES stellar libraries using the Levenberg Marquardt minimisation method (Markwardt et al. 2009). From the measured continuums and emission line widths, Type 1 AGN were selected with the following criteria:

- $0.00 < z < 0.20$
- FWHM of $H\alpha > 800$ km s^{-1}
- A/N of broad $H\alpha > 3$

This resulted in a sample of 9,671 type 1 AGN identified by Oh et al. (2015) with broad line and luminosity measurements provided in the published cataloGgue. This sample was then matched to the GZ2-STARPY sample to give 984 galaxies currently hosting AGN. This will be referred to as the AGN-HOST sample.

As the optical and NUV photometry are used to predict the most likely star formation history model of these galaxies, the flux contribution from the AGN at the centre of each galaxy had to be removed from the overall petrosian flux to give only the stellar contribution. This becomes an obvious method when the bright central point sources of the AGN in each galaxy of Figure 1 are noted.

This was achieved using the petrosian and SF magnitudes provided by SDSS and the 'AUTO' and 'aperture 3' magnitudes provided by GALEX. The GALEX PSF size is quoted at $5-6''$ therefore in order to ensure that the entirety of the flux contribution from the AGN was removed the larger $7''$ 'aperture 3' was selected (as opposed to the smaller $4.5''$ 'aperture 2' provided by GALEX). A check was made to ensure that this 7" aperture did not encompass the entire galaxy using the SDSS u-band Petrosian 90% Flux Radius, doubled to give a more accurate size of the galaxy due to the effects of the AGN point source on the Petrosian Flux estimation. 17% of the AGN host galaxies appeared to lay below this 7" radius, however upon inspection were the most luminous AGN causing the most difficulties for the Petrosian fit. Further visual inspection of the size ensured they were in fact larger than 7".

The newly corrected stellar contribution only magnitudes were k-corrected to $z = 0$ with the routine provided in Chilingarian et al. (2010) and extinction corrected using the dust maps of Schlegel et al. (1998)[3] and optical and NUV $A/E(B-V)$ values from Schlafly & Finbeiner (2011) and Seibert et al. (2005) respectively. The colours calculated from these corrected magnitudes are shown in Figure 2 in comparison to those of the GZ2-STARPY inactive galaxy sample. We can see that the AGN host galaxies typically lie between the red sequence and blue cloud populations of galaxies in the area commonly known as the green valley, an observation that also supports the findings of Cowie & Barger (2008); Hickox et al. (2009) & Schawinski et al. (2010).

This sample is studied in three different mass bins with 112 (11%) low mass ($M_* < 10.25\ M_\odot$), 572 (58%) medium mass ($10.25 < M_*[M_\odot] < 10.75$) and 300 (31%) high mass ($M_* > 10.75\ M_\odot$) galaxies and is compared to the larger GZ2-STARPY sample of 125,332 majority inactive galaxies in the three different mass bins defined above, with 41,698 (33%) low mass, 47,391 (38%) medium mass and 36,243 (29%) high mass galaxies.

The GZ2-STARPY will contain some obscured AGN, Seyfert's, LINERS etc. however these types of active galaxies are a minimal proportion of the galaxy population. Due to the high numbers of galaxies in this sample, the effects of these galaxies will get washed out and the 'typical' galaxy representative of each population will dominate the likelihoods of the population SFHs. To remove them completely with a BPT diagram would have also removed quiescent galaxies and given a sample of purely star forming galaxies which would not be representative of the galaxy population.

[3] Software for extracting the $E(B-V)$ values from the Schlegel et al. (1998) dust maps is available at `github.com/rjsmethurst/ebvpy`

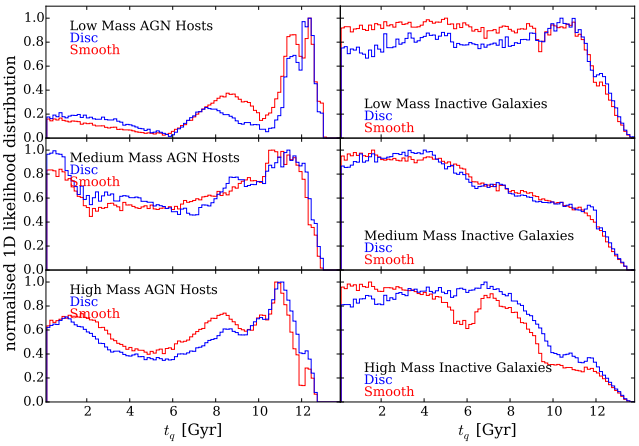

Figure 3. 1D summed distribution of 2D likelihood in quenching time for AGN (left) host and inactive (right) galaxies, split into low (top), medium (middle) and high (bottom) mass galaxies for smooth (red) and disc (blue) galaxies. A low value of t_q corresponds to the early Universe and a high value to the recent Universe.

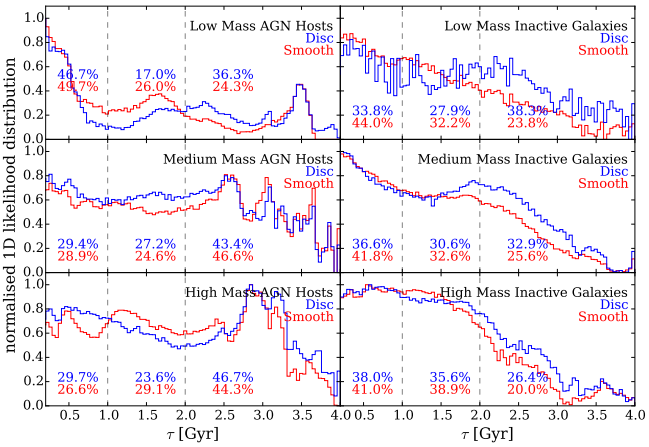

Figure 4. 1D summed distribution of 2D likelihood in quenching rate for AGN (left) host and inactive (right) galaxies, split into low (top), medium (middle) and high (bottom) mass galaxies for smooth (red) and disc (blue) galaxies. The dashed lines show the separation between rapid ($\tau < 1.0$ Gyr), intermediate ($1.0 < \tau$ [Gyr] < 2.0) and slow ($\tau > 2.0$ Gyr) quenching timescales with the fraction of the likelihood distribution in each region shown. A small (large) value of τ corresponds to a rapid (slow) quenching rate.

3 RESULTS

Each galaxy was run through STARPY to obtain a 2D likelihood distribution across the $[t_q, \tau]$ parameter space. The individual likelihood distributions of each galaxy were combined across the three mass bins defined in Secition 2.3 for AGN host and inactive galaxies. We also utilise the GZ2 morphologies and weight by the vote fractions to split the sample into smooth and disc dominated populations. We stress that this portion is purely for visualisation purposes and is no longer a Bayesian method.

These 2D likelihoods are summed across each parame-

ter axis and normalised to produce the one dimensional histograms shown in Figures 3 and 4 for the quenching time, t_q and quenching rate τ respectively. In each figure the summed 1D normalised probability distribution across the given parameter is shown for smooth (red) and disc (blue) galaxies split into the three mass bins; low (top), medium (middle) and high (bottom) mass galaxies for the AGN host (left) and inactive galaxies (right). In Figure 4 the percentage likelihood in each region of quenching rate shown by the dashed lines for rapid ($\tau < 1$ Gyr), intermediate ($1 < \tau$ [Gyr] < 2) and slow ($\tau > 2$ Gyr) quenching timescales.

It is immediately apparent from Figures 3 and 4 that there is a distinct difference between the distribution of likelihood for AGN hosts (left panels) and inactive galaxies (right panels) for both parameters. For the inactive galaxies, the likelihood for quenching at later times decreases with increasing mass, whereas for the lower mass galaxies the quenching is roughly constant with time for both smooth and disc dominated populations. This is observational evidence of downsizing across the generic galaxy population whereby stars in massive galaxies form first and subsequent star formation at later times is suppressed therefore there is no star formation to quench (Cowie et al. 1996; Thomas et al. 2010).

The distribution of likelihood for AGN host galaxies across the quenching time t_q parameter (left panels of Figure 3), is very obviously different from that of the inactive galaxies (right panels of Figure 3). Recent quenching is the most dominant history across all three mass bins, particularly for low mass galaxies. However, this effect is dampened in higher mass galaxies where quenching at earlier times also has significant likelihood.

The distribution of likelihoods for the rate of quenching, τ parameter, in Figure 4, show once again the AGN host (left panels) and inactive (right panels) galaxies distributions are vastly different. The likelihood for rapid quenching ($\tau <$ 1 Gyr) increases for inactive galaxies of increasing mass (see percentage likelihoods in the left hand panels of Figure 4). The likelihood for slow quenching ($\tau > 2$ Gyr) also increases for inactive disc galaxies with increasing mass.

However, the distribution of likelihood of the rate of quenching for the AGN host galaxies is in fact the opposite to that seen for inactive galaxies. The likelihood for rapid quenching decreases with increasing mass for both smooth and disc dominated populations and conversely for slow quenching rates increases with increasing mass disc galaxies quenching timescales.

4 DISCUSSION

The vast differences between the distribution of likelihood for the AGN host and inactive galaxy populations reveals that AGN have a significant effect on the SFH of their host galaxy and can be associated with both recent rapid quenching and earlier, slower quenching histories.

As well as the clear evidence for downsizing in the inactive galaxy population from Figure 3 we can also see it's effect on the AGN host galaxies. Although recent quenching is the dominant history, quenching at earlier times also has significant likelihood with increasing mass. These galaxies may have undergone downsizing earlier in life with the current AGN also having an effect on the SFR through feedback, causing a recent, rapid quench of any residual star formation.

If a slowly 'dying' or 'dead' galaxy has an infall of gas either through a minor merger, galaxy interaction or environmental change, this can trigger further star formation and feed the central black hole, igniting an AGN. In turn this AGN can then quench the recent boost in star formation. This track is similar to the evolution history theorised for blue ellipticals (Kaviraj et al. 2013; McIntosh et al. 2014; Haines et al. 2015). As for the disc galaxies, it also follows from the ideas of previously isolated discs evolving slowly by the Kennicutt-Schmidt (KS; Schmidt 1959; Kennicutt 1997) law which may then undergo an interaction or merger to reinvigorate star formation and feed the central black hole.

The difference between the AGN host and inactive galaxies distribution of likelihood in Figure 4 for the rate of quenching, τ parameter tells a story of gas reservoirs. Smethurst et al. (2015) speculated that rapid quenching rates could be attributed to mergers of galaxies, therefore we expect the trend of increasing likelihood for rapid quenching rates with increasing mass for the inactive galaxies, as mergers are thought to be responsible for creating the most massive smooth galaxies (Conselice et al. 2003; Springel, Di Matteo & Hernquist 2005; Hopkins et al. 2008). Similarly we also expect the trend of increasing likelihood for slow quenching rates with increasing mass as Smethurst et al. (2015) attributed slower quenching histories to secular (non-violent) evolution of isolated galaxies (Kormendy & Kennicutt 2004; Cisternas et al. 2011) which are often lower in mass (Varela et al. 2004; Bamford et al. 2009) due to their isolation from other galaxies and therefore any potential gas reservoirs.

The trends with likelihood of τ in Figure 4 are reversed however for the AGN host galaxies. The likelihood for rapid quenching decreases with increasing mass for both smooth and disc dominated populations and for slow quenching increases with increasing mass disc galaxies. It appears that the most massive disc galaxies, therefore with the most massive gas reservoirs evolve with a slow quench of star formation through the KS law and also have enough gas to feed the central black hole to trigger a current AGN (Varela et al. 2004; Emsellem et al. 2015). Conversely, a rapid quench, possibly caused by the AGN itself through negative feedback, is only the most dominant history for low mass galaxies with lower gravitational potentials which allow gas to be expelled more easily (or heated by the AGN) across the entire galaxy (Tortora et al. 2009). This rapid quenching is still apparent but at a lower likelihood across the smooth and disc populations in higher mass galaxies, with larger potentials, which make it more difficult for the AGN to have an impact on the galaxy wide SFR (Ishibashi et al. 2012; Zinn et al. 2013).

We have used morphological classifications from the Galaxy Zoo 2 project to determine the morphology-dependent star formation histories of AGN host and inactive galaxies via a Bayesian analysis of an exponentially declining star formation quenching model. We determined the most likely parameters for the quenching onset time, t_q and quenching timescale τ to look for differences in the combined population likelihoods between inactive and AGN host galaxies. We find evidence for a link between a galaxy currently hosting an AGN and the SFR. There is a clear

difference between the likelihood distributions of AGN host and inactive galaxies and we find evidence of downsizing in massive inactive galaxies, which appears as a secondary effect in AGN host galaxies with the dominant quenching occurring at recent times. There is also evidence of negative feedback from AGN in lower mass galaxies from dominant rapid quenching tracks.

ACKNOWLEDGEMENTS

RS acknowledges funding from the Science and Technology Facilities Council Grant Code ST/K502236/1. BDS gratefully acknowledges support from the Oxford Martin School, Worcester College and Balliol College, Oxford. KS gratefully acknowledges support from Swiss National Science Foundation Grant PP00P2_138979/1.

The development of Galaxy Zoo was supported in part by the Alfred P. Sloan Foundation. Galaxy Zoo was supported by The Leverhulme Trust.

Based on observations made with the NASA Galaxy Evolution Explorer. GALEX is operated for NASA by the California Institute of Technology under NASA contract NAS5-98034

Funding for the SDSS and SDSS-II has been provided by the Alfred P. Sloan Foundation, the Participating Institutions, the National Science Foundation, the U.S. Department of Energy, the National Aeronautics and Space Administration, the Japanese Monbukagakusho, the Max Planck Society, and the Higher Education Funding Council for England. The SDSS Web Site is `http://www.sdss.org/`. The SDSS is managed by the Astrophysical Research Consortium for the Participating Institutions. The Participating Institutions are the American Museum of Natural History, Astrophysical Institute Potsdam, University of Basel, University of Cambridge, Case Western Reserve University, University of Chicago, Drexel University, Fermilab, the Institute for Advanced Study, the Japan Participation Group, Johns Hopkins University, the Joint Institute for Nuclear Astrophysics, the Kavli Institute for Particle Astrophysics and Cosmology, the Korean Scientist Group, the Chinese Academy of Sciences (LAMOST), Los Alamos National Laboratory, the Max-Planck-Institute for Astronomy (MPIA), the Max-Planck-Institute for Astrophysics (MPA), New Mexico State University, Ohio State University, University of Pittsburgh, University of Portsmouth, Princeton University, the United States Naval Observatory, and the University of Washington.

This publication made extensive use of the Tool for Operations on Catalogues And Tables (TOPCAT; Taylor 2005) which can be found at `http://www.star.bris.ac.uk/~mbt/topcat/`. Ages were calculated from the observed redshifts using the *cosmolopy* package provided in the Python module *astroPy*[4]; Robitaille et al. 2013). This research has also made use of NASA's ADS service and Cornell's ArXiv.

REFERENCES

Aihara, H. et al., 2011, ApJSS, 193, 29
Bamford, S. et al., 2009, MNRAS, 393, 1324
Bower, R. et al., 2006, MNRAS, 370, 645
Bruzual, G. & Charlot, S., 2003, MNRAS, 344, 1000
Chilingarian, I. V. et al., 2010, MNRAS, 405, 1409
Cisternas, M. et al., 2011, ApJ, 726, 57
Conselice, C. J. et al., 2003, AJ, 126, 1183
Cowie, L. et al., 1996, AJ, 112, 839
Cowie, L. & Barger, A. J., 2008, ApJ, 686, 72
Croton, D. J. et al., 2006, MNRAS, 365, 11
Emsellem, E. et al. 2015, MNRAS, 446, 2468
Fabian, A. C. 2006, ARA&A, 50, 455
Haines, T. et al., 2015, arXiv:1505.01493
Haring, N. & Rix, H-W., 2004, ApJ, 604, 89
Hickox, R. C., et al., 2009, ApJ, 696, 891
Hopkins, F. et al., 2008, ApJSS, 175, 390
Ishibashi, W. et al., 2012, MNRAS, 427, 2998
Kaviraj, S. et al., 2013, MNRAS, 428, 925
Kennicutt, R. C., 1997, ApJ, 498, 491
Kormendy, J. & Kennicutt, R. J., 2004, ARA&A, 42, 603
Lintott, C. J. et al., 2008, MNRAS, 389, 1179
Lintott, C. J. et al., 2011, MNRAS, 410, 166
Magorrian, J. et al., 1998, AJ, 115, 2285
Marconi, A. & Hunt, L. K., 2003, ApJ, 589, 21
Markwardt, C. B. 2009, in Astronomical Society of the Pacific Conference Series, Vol. 411, Astronomical Data Analysis Software and Systems XVIII, ed. D. A. Bohlender, D. Durand & P. Dowler, 251
McIntosh, D. et al., 2014, MNRAS, 442, 533
Oh, K., Sarzi, M., Schawinski, K., & Yi, S. K., 2011, ApJS, 195, 13
arXiv: 1504.07247
Robitaille, T. P. et al., 2013, A&A, 558, A33
Sarzi, M. et al., 2006, MNRAS, 366, 1151
Schawinski, et al., 2007, MNRAS, 382, 1415
Schawinski, K. et al., 2010, MNRAS, 711, 284
Schlafly & Finkbeiner, 2011, ApJ, 737, 103
Schlegel, D. J. et al., 1998, ApJ, 500, 523
Schmidt, M., 1959, ApJ, 129, 243
Seibert et al., 2005, ApJ, 619, L55
Smethurst, R. J. et al., 2015, MNRAS, 450, 435
Somerville, R. S. et al., 2008, MNRAS, 391, 481
Springel, V., Di Matteo, T. & Hernquist, L., 2005, ApJ, 620, L79
Taylor, M. B., 2005, ASP Conference Series, 347
Thomas, D. et al., 2010, MNRAS, 404, 1775
Tortora, C. et al., 2009, MNRAS, 369, 61
Varela, J. et al., 2004, A&A, 420, 873
Willett, K. et al., 2013, MNRAS, 435, 2835
York, D. G. et al., 2000, AJ, 120, 1579
Zinn, P. et al., 2013, ApJ, 774, 66

[4] `http://www.astropy.org/`